Geometric Derivation and Analysis of Multi-Symplectic Numerical Schemes for Differential Equations

Odysseas Kosmas, Dimitrios Papadopoulos, and Dimitrios Vlachos

Abstract In the current work we present a class of numerical techniques for the solution of multi-symplectic PDEs arising at various physical problems. We first consider the advantages of discrete variational principles and how to use them in order to create multi-symplectic integrators. We then consider the nonstandard finite difference framework from which these integrators derive. The latter is now expressed at the appropriate discrete jet bundle, using triangle and square discretization. The preservation of the discrete multi-symplectic structure by the numerical schemes is shown for several one- and two-dimensional test cases, like the linear wave equation and the nonlinear Klein–Gordon equation.

1 Introduction and Motivation

In general, symplectic integrators are robust, efficient, and accurate in preserving the long time behavior of the solutions of Hamiltonian ordinary differential equations (ODEs) [1]. The basic feature of a symplectic integrator is that the numerical performance is designed to preserve a physical observable property, i.e., the symplectic form at each time step. Recently, it was shown that many conservative partial differential equations (PDEs) allow for description similar to the symplectic structure of Hamiltonian ODEs, called the multi-symplectic formulation (see, e.g., Refs. [2–5]). For example, in Ref. [2] the authors develop the multi-symplectic

O. Kosmas (✉)
Modelling and Simulation Centre, MACE, University of Manchester, Manchester, UK
e-mail: odysseas.kosmas@manchester.ac.uk

D. Papadopoulos
Delta Pi Systems Ltd., Thessaloniki, Greece
e-mail: dimitris@delta-pi-systems.eu

D. Vlachos
Department of Informatics & Telecommunications, University of Peloponnese, Tripoli, Greece
e-mail: dvlachos@uop.gr

N. J. Daras, T. M. Rassias (eds.), *Computational Mathematics and Variational Analysis*, Springer Optimization and Its Applications 159,
https://doi.org/10.1007/978-3-030-44625-3_12

structure of Hamiltonian PDEs from a Lagrangian formulation, using the variational principle. The wave equation and its multi-symplectic structure have been studied by [6–8] from the Hamiltonian viewpoint.

On the other hand, in the past decades, nonstandard finite difference schemes have been well established by Mickens [9–11] to compensate the weaknesses that may be caused by standard finite difference methods, such as the numerical instabilities. Regarding the positivity, the boundedness, and the monotonicity of solutions, nonstandard finite difference schemes have a better performance than standard ones, due to their flexibility to construct a nonstandard finite difference method. The latter can preserve certain properties and structures, which are obeyed by the original equations.

In the present paper, following our previous work [12] we pay special attention to the geometric structure of multi-symplectic integrators through the use of nonstandard finite difference schemes for variational partial differential equations (PDEs). The considered approach comes as a first step towards developing a Veselov type discretization for PDEs in variational form, e.g., [2, 4, 5] and combines it with nonstandard finite difference schemes of Mickens [9–11]. The resulting multisymplectic-momentum integrators have very good energy performance in the level of the conservation of a nearby Hamiltonian, under appropriate circumstances, up to exponentially small error [2].

In Section 2 we present a short overview of the standard numerical techniques relying on variational integrator schemes and their special case of exponential variational integrators in Section 3. Afterwards, nonstandard finite difference properties are employed for the derivation of nonstandard variational integrators by using a triangle discretization of the spacetime (Section 4.1). Then, in Sections 5 and 6, we demonstrate concrete applications of the proposed integrators, for the numerical solution of the linear wave equation, the Laplace equation, and the Poisson equation. In Section 7, we perform dispersion analysis and convergence experiments to further illustrate the numerical properties of the method. Finally, in Section 8, we summarize the main conclusions coming out of our study.

2 Review of Variational Integrators

The discrete Euler–Lagrange equations can be derived in correspondence to the steps of derivation of the Euler–Lagrange equations in the continuous formulation of Lagrangian dynamics [3]. Denoting the tangent bundle of the configuration manifold Q by TQ, the continuous Lagrangian $L : TQ \to \mathbb{R}$ can be defined. In the discrete setting, considering approximate configurations $q_k \approx q(t_k)$ and $q_{k+1} \approx q(t_{k+1})$ at the time nodes t_k, t_{k+1}, with $h = t_{k+1} - t_k$ being the fixed time step, a discrete Lagrangian $L_d : Q \times Q \to \mathbb{R}$ is defined to approximate the action integral along the curve segment between q_k and q_{k+1}, i.e.,

$$L_d(q_k, q_{k+1}) \approx \int_{t_k}^{t_{k+1}} L(q(t), \dot{q}(t))dt. \tag{1}$$

Defining the discrete trajectory $\gamma_d = (q_0, \ldots, q_N)$, $N \in \mathbb{N}$, one can obtain the action sum

$$S_d(\gamma_d) = \sum_{k=1}^{N-1} L_d(q_k, q_{k+1}). \tag{2}$$

The discrete Hamilton's principle states that a motion γ_d of the discrete mechanical system extremizes the action sum, i.e., $\delta S_d = 0$. Through differentiation and rearrangement of the terms, holding the end points q_0 and q_N fixed, the discrete Euler–Lagrange equations are obtained [3]

$$D_2 L_d(q_{k-1}, q_k) + D_1 L_d(q_k, q_{k+1}) = 0, \quad k = 1, \ldots, N-1, \tag{3}$$

where the notation $D_i L_d$ indicates derivative with respect to the i-th argument of L_d, see also [3, 12–16].

The definition of the discrete conjugate momentum at time steps k and $k+1$ reads

$$p_k = -D_1 L_d(q_k, q_{k+1}), \quad p_{k+1} = D_2 L_d(q_k, q_{k+1}), \quad k = 0, \ldots, N-1. \tag{4}$$

The above equations, also known as position–momentum form of a variational integrator, can be used when an initial condition (q_0, p_0) is known, to obtain (q_1, p_1).

To construct high order methods, we approximate the action integral along the curve segment between q_k and q_{k+1} using a discrete Lagrangian that depends only on the end points. We obtain expressions for configurations q_k^j and velocities $\dot{q}_k^j$ for $j = 0, \ldots, S-1$, $S \in \mathbb{N}$ at time $t_k^j \in [t_k, t_{k+1}]$ by expressing $t_k^j = t_k + C_k^j h$ for $C_k^j \in [0, 1]$ such that $C_k^0 = 0$, $C_k^{S-1} = 1$ using

$$q_k^j = g_1(t_k^j) q_k + g_2(t_k^j) q_{k+1}, \qquad \dot{q}_k^j = \dot{g}_1(t_k^j) q_k + \dot{g}_2(t_k^j) q_{k+1}, \tag{5}$$

where $h \in \mathbb{R}$ is the time step. We choose functions

$$g_1(t_k^j) = \sin\left(u - \frac{t_k^j - t_k}{h} u\right) (\sin u)^{-1}, \quad g_2(t_k^j) = \sin\left(\frac{t_k^j - t_k}{h} u\right) (\sin u)^{-1}, \tag{6}$$

to represent the oscillatory behavior of the solution, see [17, 18]. For continuity, $g_1(t_{k+1}) = g_2(t_k) = 0$ and $g_1(t_k) = g_2(t_{k+1}) = 1$ is required.

For any different choice of interpolation used, we define the discrete Lagrangian by the weighted sum

$$L_d(q_k, q_{k+1}) = h \sum_{j=0}^{S-1} w^j L(q(t_k^j), \dot{q}(t_k^j)), \tag{7}$$

where it can be easily proved that for maximal algebraic order

$$\sum_{j=0}^{S-1} w^j (C_k^j)^m = \frac{1}{m+1}, \tag{8}$$

where $m = 0, 1, \ldots, S-1$ and $k = 0, 1, \ldots, N-1$, see [17, 18].

Applying the above interpolation technique with the trigonometric expressions of (6), following the phase lag analysis of [13, 14, 17, 18], the parameter u can be chosen as $u = \omega h$. For problems that include a constant and known domain frequency ω (such as the harmonic oscillator) the parameter u can be easily computed. For the solution of orbital problems of the general N-body problem, where no unique frequency is given, a new parameter u must be defined by estimating the frequency of the motion of any moving point mass [16, 19–21].

3 Exponential Integrators

We now consider the Hamiltonian systems

$$\ddot{q} + \Omega q = g(q), \qquad g(q) = -\nabla U(q), \tag{9}$$

where Ω is a diagonal matrix (will contain diagonal entries ω with large modulus) and $U(q)$ is a smooth potential function. We are interested in the long time behavior of numerical solutions when ωh is not small.

Since $q_{n+1} - 2\cos(h\omega)q_n + q_{n-1} = 0$ is an exact discretization of (9) we can consider the numerical scheme

$$q_{n+1} - 2\cos(h\omega)q_n + q_{n-1} = h^2 \psi(\omega h) g(\phi(\omega h) q_n), \tag{10}$$

where the functions $\psi(\omega h)$ and $\phi(\omega h)$ are even, real-valued functions satisfying $\psi(0) = \phi(0) = 1$, see [1]. The resulting methods using the latter numerical scheme are known as exponential integrators (for some examples of those integrators, see the Appendix).

3.1 Exponential High Order Variational Integrators

If we now use the phase fitted variational integrator for the system (9) the result of the discrete Euler–Lagrange equations (3) will be

$$q_{n+1} + \Lambda(u, \omega, h, S)q_n + q_{n-1} = h^2\Psi(\omega h)g(\Phi(\omega h)q_n), \tag{11}$$

where

$$\Lambda(u, \omega, h, S) = \frac{\sum_{j=0}^{S-1} w^j \left[\dot{g}_1(t_k^j)^2 + \dot{g}_2(t_k^j)^2 - \omega^2 \left(g_1(t_k^j)^2 + g_2(t_k^j)^2 \right) \right]}{\sum_{j=0}^{S-1} w^j \left[\dot{g}_1(t_k^j)\dot{g}_2(t_k^j) - \omega^2 g_1(t_k^j) g_2(t_k^j) \right]}. \tag{12}$$

Using the above expressions, to obtain exponential variational integrators that use expressions for configurations q_k^j and velocities $\dot{q}_k^j$ taken from (5), we get

$$\Lambda(u, \omega, h, S) = -2\cos(\omega h). \tag{13}$$

In [16] we have proved (using the phase lag analysis of [22]) that exponentially fitted methods using phase fitted variational integrators can be derived when (13) holds. So phase fitted variational integrators using trigonometric interpolation can be considered as exponential integrators, i.e., when using phase fitted variational integrators, keeping the phase lag zero the resulting methods are exponentially fitted methods (exponential integrators). Those methods have been tested on several numerical results in [16].

3.2 Frequency Estimation for Mass Points Motion in Three Dimensions

In our previous work [16], we constructed adaptive time step variational integrators using phase fitting techniques and estimated the required frequency through the use of a harmonic oscillator with given frequency ω. Here, in solving the general N-body problem by using a constant time step, a new frequency estimation is necessary in order to find for each body i) the frequency at an initial time t_0 and ii) the frequency at time t_k for $k = 1, \ldots, N-1$.

It is now clear that, by applying the trigonometric interpolation (6), the parameter u can be chosen as $u = \omega h$. For problems for which the domain of frequency ω is fixed and known (such as the harmonic oscillator) the parameter u can be easily computed. For the solution of orbital problems involved in the general N-body

problem, where no unique frequency is determined, the parameter u must be defined by estimating the frequency of the motion of any moving material point.

Towards this purpose, we consider the general case of N masses moving in three dimensions. If $q_i(t)$ $(i = 1, \ldots, N)$ denotes the trajectory of the i-th particle, its curvature can be computed from the known expression

$$k_i(t) = \frac{|\dot{q}_i(t) \times \ddot{q}_i(t)|}{|\dot{q}_i(t)|^3}, \tag{14}$$

where $\dot{q}_i(t)$ is the velocity of the i-th mass with magnitude $|\dot{q}_i(t)|$ at a point $q_i(t)$. After a short time h, the angular displacement of that mass is $h|\dot{q}_i(t) \times \ddot{q}_i(t)|/|\dot{q}_i(t)|^2$, which for each mass's actual frequency gives the expression

$$\omega_i(t) = \frac{|\dot{q}_i(t) \times \ddot{q}_i(t)|}{|\dot{q}_i(t)|^2}. \tag{15}$$

From (14) and (15) the well-known relation $\omega_i(t) = k_i(t)|\dot{q}_i(t)|$ holds (see also [16]).

For the specific case of many-particle physical problems, that can be described via a Lagrangian of the form $L(q, \dot{q}) = \frac{1}{2}\dot{q}^T M(q)\dot{q} - V(q)$, where $M(q)$ represents a symmetric positive definite mass matrix and V is a potential function, the continuous Euler–Lagrange equations are $M(q)\ddot{q} = -\nabla V(q)$. In this case, the expression for frequency estimation (15), referred to the i-th body at time t_k, $k = 1, \ldots, N-1$, takes the form

$$\omega_i(t_k) = h^{-1} \frac{\left|M^{-1}(q_k)p_k \times \left(M^{-1}(q_k)p_k - M^{-1}(q_{k-1})p_{k-1}\right)\right|}{\left|M^{-1}(q_k)p_k\right|^2}, \tag{16}$$

where the quantities on the right-hand side are the mass matrix, the configuration, and the momentum of the i-th body. Since the frequency $\omega_i(t_k)$ must be also known at an initial time instant t_0 (in which the initial positions are $\bar{q}_0$ and initial momenta are $\bar{p}_0$), using the continuous Euler–Lagrange equation at t_0 we obtain

$$\omega_i(t_0) = \frac{\left|M^{-1}(\bar{q}_0)\bar{p}_0 \times \left(-M^{-1}(\bar{q}_0)\nabla V(\bar{q}_0)\right)\right|}{\left|M^{-1}(\bar{q}_0)\bar{p}_0\right|^2}. \tag{17}$$

Equations (16) and (17) provide an "estimated frequency" for each mass in the general motion of the N-body problem. This allows us to derive high order variational integrator methods using trigonometric interpolation where the frequency is estimated at every time step of the integration procedure. These methods show better energy behavior, i.e., smaller total energy oscillation than other methods which employ constant frequency, see [14, 16].

Before closing this section, it should be mentioned that the linear stability of our method is comprehensively analyzed in our previous works [14, 16, 19].

4 Triangle and Square Discretization

In order to express the discrete Lagrangian and discrete Hamilton function, we will use the definition of the tangent bundle TQ and cotangent bundle T^*Q as in [2] to fields over the higher-dimensional manifold X. In this way, we also view fields over X as sections of some fiber bundle $B \to X$, with fiber Y, and then consider the first jet bundle J^1B and its dual (J^1B^*) as the appropriate analogs of the tangent and cotangent bundles.

It is then possible to use the generalization of the Veselov discretization [4, 5] to multi-symplectic field theory, by discretizing the spacetime X. For simplicity reasons we will restrict ourselves to the discrete analogue of $\dim X = 2$. Thus, we take $X = \mathbb{Z} \times \mathbb{Z} = (i, j)$ and the fiber bundle Y to be $X \times F$ for some smooth manifold F [2, 12].

4.1 Triangle Discretization

Assume that we have a uniform quadrangular mesh in the base space, with mesh lengths Δx and Δt. The nodes in this mesh are denoted by $(i, j), \in \mathbb{Z} \times \mathbb{Z}$, corresponding to the points $(x_i, t_j) := (i\Delta x, j\Delta t) \in \mathbb{R}^2$. We denote the value of the field u at the node (i, j) by u^i_j. We label the triangle at (i, j) with three ordered triple $((i, j), (i+1, j), (i, j+1))$ as $\triangle_{ij}$, and we define $X_\triangle$ to be the set of all such triangles, see Figure 1.

Then, the discrete jet bundle is defined as follows [2]:

$$J^1_\triangle Y := \{(u^j_i, u^j_{i+1}, u^{j+1}_i) \in \mathbb{R}^3 : ((i, j), (i+1, j), (i, j+1)) \in X_\triangle\}, \tag{18}$$

which is equal to $X_\triangle \times \mathbb{R}^3$. The field u can be now defined by averaging the fields over all vertices of the triangle (see Figure 1a)

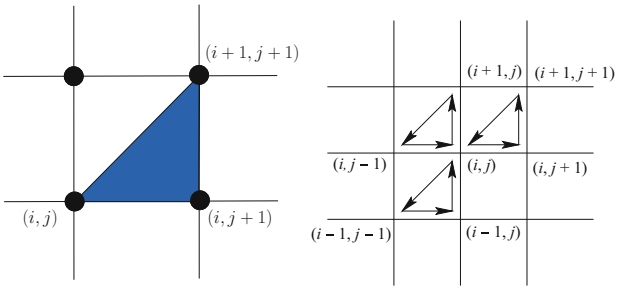

Fig. 1 The triangles which touch (i, j)

$$u \to \frac{u_i^j + u_i^{j+1} + u_{i+1}^{j+1}}{3}, \tag{19}$$

while the derivatives can be expressed using nonstandard finite differences [9–11]

$$\frac{du}{dt} \to \frac{u_i^{j+1} - u_i^j}{\phi(\Delta t)}, \qquad \frac{du}{dx} \to \frac{u_{i+1}^{j+1} - u_i^{j+1}}{\psi(\Delta x)}, \tag{20}$$

with [9, 10]

$$\phi(\Delta t) = 2\sin\left(\frac{\Delta t}{2}\right), \quad \psi(\Delta x) = 2\sin\left(\frac{\Delta x}{2}\right). \tag{21}$$

Using the latter expressions, we can obtain the discrete Lagrangian at any triangle, which depends on the edges of the triangle, i.e., $L_d(u_i^j, u_i^{j+1}, u_{i+1}^{j+1})$, while the discrete Euler–Lagrange field equations are

$$D_1 L_d(u_i^j, u_i^{j+1}, u_{i+1}^{j+1}) + D_2 L_d(u_i^{j-1}, u_i^j, u_{i+1}^j) + D_3 L_d(u_{i-1}^{j-1}, u_{i-1}^j, u_i^j) = 0, \tag{22}$$

see Figure 1 (right).

4.2 Square Discretization

For the cases where square discretization is used, and if we also denote a square at (i, j) with four ordered quaternion $((i, j), (i + 1, j), (i + 1, j + 1), (i, j + 1))$ by $\square_j^i$, we can consider $X_\square$ to be the set of all such squares, see Figure 1. Then, the discrete jet bundle is defined as (for more details see [2] and the references therein)

$$J^1_\square Y := \Big\{ (u_i^j, u_{i+1}^j, u_{i+1}^{j+1}, u_i^{j+1}) \in \mathbb{R}^4 : ((i, j), (i+1, j), (i+1, j+1), (i, j+1)) \in X_\square \Big\}, \tag{23}$$

which is equal to $X_\square \times \mathbb{R}^4$.

By averaging the fields over all vertices of the square, the field u can be now obtained as (see Figure 2 (left))

$$u \to \frac{u_i^j + u_{i+1}^j + u_i^{j+1} + u_{i+1}^{j+1}}{4}. \tag{24}$$

As above, the expressions for the derivatives can be taken from [9–11] for the discrete Lagrangian, which now depends on the edges of the square, i.e., $L_d(u_i^j, u_{i+1}^j, u_{i+1}^{j+1}, u_i^{j+1})$. As a result, the discrete Euler–Lagrange field equations are

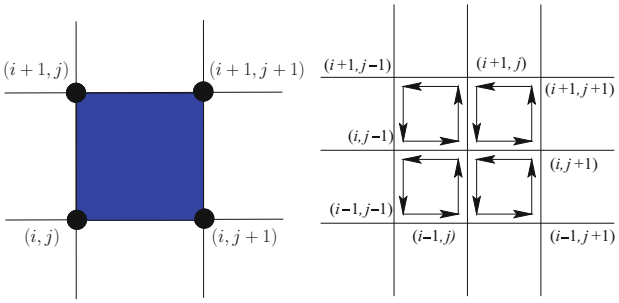

Fig. 2 The squares which touch (i, j)

$$D_1 L_d(u_i^j, u_i^{j+1}, u_{i+1}^{j+1}, u_{i+1}^j) + D_2 L_d(u_i^{j-1}, u_i^j, u_{i+1}^j, u_{i+1}^{j-1}) +$$
$$D_3 L_d(u_{i-1}^{j-1}, u_{i-1}^j, u_i^j, u_i^{j-1}) + D_4 L_d(u_{i-1}^j, u_{i-1}^{j+1}, u_i^{j+1}, u_i^j) = 0, \tag{25}$$

see Figure 2 (right).

5 Numerical Examples Using Triangle Discretization

To illustrate the proposed method, we consider the basic PDEs of three physical problems, i.e., the linear wave equation, the Laplace equation, and the Poisson equation (see [2] and [23, 24]). In the following subsections, for representation requirements, quadrilaterals have been used by interpolating the solution on triangles.

5.1 Linear Wave Equation

The linear wave equation contains second-order partial derivatives of the wave function $u(x, t)$ with respect to time and space, respectively, as (see, e.g., [23, 24])

$$\frac{\partial^2 u}{\partial t^2} + c\frac{\partial^2 u}{\partial x^2} = 0. \tag{26}$$

This equation may be considered for the description of the wave function, i.e., the amplitude of oscillation, that is created from a one-dimensional medium (e.g., a string extended in the x-direction). For the special case that the velocity of the wave, representing by the parameter c, is chosen as $c = -1$, the corresponding Lagrangian is [12]

$$L(u, u_t, u_x) = \frac{1}{2}u_t^2 - \frac{1}{2}u_x^2, \tag{27}$$

where the derivatives are $\partial u/\partial t = u_t$ and $\partial u/\partial x = u_x$.

If we use triangle discretization, described in Section 4.1, we end up with discrete Lagrangian

$$L_d\left(u_i^j, u_i^{j+1}, u_{i+1}^{j+1}\right) = \frac{1}{2}\Delta t \Delta x \left[\frac{1}{2}\left(\frac{u_i^{j+1} - u_i^j}{\phi(\Delta t)}\right)^2 - \frac{1}{2}\left(\frac{u_{i+1}^{j+1} - u_i^{j+1}}{\psi(\Delta x)}\right)^2\right], \tag{28}$$

where Δt and Δx are the mesh lengths for time and space, respectively. Applying the above discrete Lagrangian to the discrete Euler–Lagrange field equations (22), we get

$$\frac{u_i^{j+1} - 2u_i^j + u_i^{j-1}}{(\phi(\Delta t))^2} - \frac{u_{i+1}^j - 2u_i^j + u_{i-1}^j}{(\psi(\Delta x))^2} = 0. \tag{29}$$

The latter expression represents the variational integrator for the linear wave equation (26), resulting through the use of the proposed nonstandard finite difference schemes.

In Figure 3 the solution $u(x, t)$ of (29) is shown in a 3-D diagram. We have chosen as initial conditions $0 < x < 1, u(x, 0) = 0.5[1-\cos(2\pi x)], u_t(x, 0) = 0.1$ and as boundary conditions $u(0, t) = u(1, t)$, $u_x(0, t) = u_x(1, t)$, the latter being periodic. The grid discretization has been taken to be $\Delta t = 0.01$ and $\Delta x = 0.01$. As seen, the time evolution of the solution $u(x = const., t)$ is a continuous function, while the periodicity is preserved.

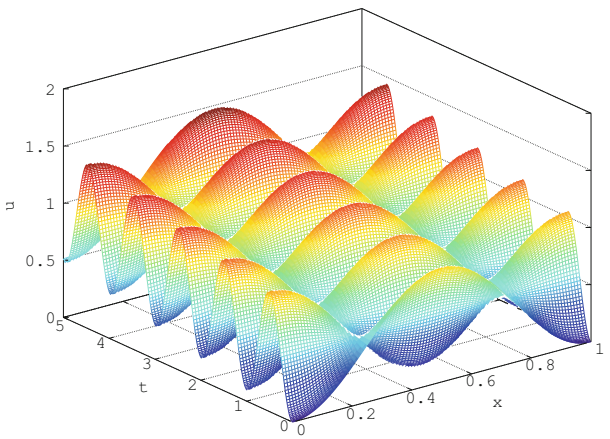

Fig. 3 The waveforms of linear wave equation (26)

5.2 Laplace Equation

As another physical example, we have chosen the Laplace equation over a 2-D scalar field $u(x, y)$. It is written as

$$u_{xx} + u_{yy} = 0. \tag{30}$$

The function $u(x, y)$ may describe a potential in a 2-D medium or a potential inside a 3-D medium, which does not depend on the third coordinate z. Thus, the two-dimensional second-order PDE (30) governs a variety of equilibrium physical phenomena such as temperature distribution in solids, electric field in electrostatics, inviscid and irrotational two-dimensional flow (potential flow), groundwater flow, etc.

The corresponding continuous Lagrangian of (30) takes the form

$$L(u, u_x, u_y) = \frac{1}{2}u_x^2 + \frac{1}{2}u_y^2. \tag{31}$$

By applying the triangle discretization of Section 4.1, the discrete Lagrangian can be written as

$$L_d\left(u_i^j, u_i^{j+1}, u_{i+1}^{j+1}\right) = \frac{1}{2}\Delta x \Delta y \left[\frac{1}{2}\left(\frac{u_i^{j+1} - u_i^j}{\phi(\Delta x)}\right)^2 + \frac{1}{2}\left(\frac{u_{i+1}^{j+1} - u_i^{j+1}}{\psi(\Delta y)}\right)^2\right]. \tag{32}$$

From the latter Lagrangian, working in a similar manner to that followed in Section 4.2 results the integrator from the proposed nonstandard finite difference schemes

$$\frac{u_i^{j+1} - 2u_i^j + u_i^{j-1}}{(\phi(\Delta x))^2} + \frac{u_{i+1}^j - 2u_i^j + u_{i-1}^j}{(\psi(\Delta y))^2} = 0. \tag{33}$$

The solution of the above equation, when considering the boundary conditions $u(x, 0) = 0$, $u(x, 1) = 1$ and $u(0, y) = u(1, y) = 0$, is plotted in Figure 4. The grid discretization has been chosen to be $\Delta x = 0.02$ and $\Delta y = 0.02$.

5.3 Poisson Equation

As a final application to illustrate the advantages of the proposed variational integrator relying on nonstandard finite difference schemes, we examine the Poisson equation, which is an elliptic PDE of the form

$$-u_{xx} - u_{yy} = f(x, y). \tag{34}$$

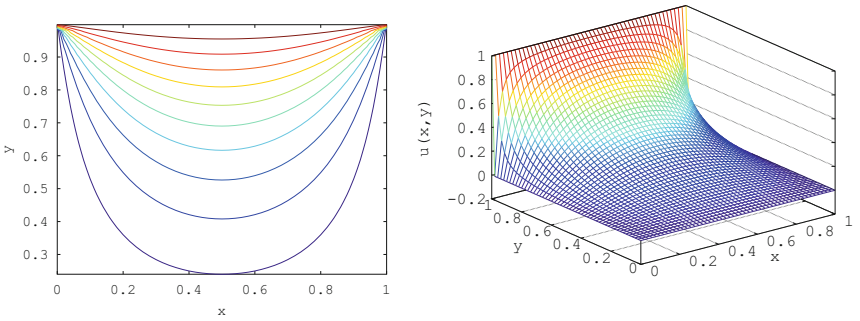

Fig. 4 Contour plot (left) and three-dimensional surface plot (right) of the solution of Laplace equation with boundary conditions $u(x, 0) = 0$, $u(x, 1) = 1$, $u(0, y) = u(1, y) = 0$, and discretization: $\Delta x = 0.02$, $\Delta y = 0.02$

Obviously, this equation in physical applications presents an additional complexity compared to the Laplace equation (30). Now the right-hand side is a nonzero function $f(x, y)$, which may be considered as a source (or a load) function defined on some two-dimensional domain denoted by $\Omega \subset \mathbb{R}^2$ (it could also be a general nonlinear function $f(u, x, y)$). A solution u satisfying (34) will also satisfy specific conditions on the boundaries of the domain Ω. For example, for the element $\partial\Omega$ the general condition holds

$$\alpha u + \beta \frac{\partial u}{\partial n} = g \qquad \text{on} \quad \partial\Omega, \tag{35}$$

where $\partial u/\partial n$ denotes the directional derivative in the direction normal to the boundary $\partial\Omega$ and α and β are constants [23, 24].

As it is well known, the system of (34) and (35) is referred to as a boundary value problem for the Poisson equation. If the constant β in Equation (35) is zero, then the boundary condition is of Dirichlet type, and the boundary value problem is referred to as the Dirichlet problem for the Poisson equation. Alternatively, if the constant α is zero, then we correspondingly have a Neumann boundary condition, and the problem is referred to as a Neumann problem. A third possibility exists when the Dirichlet conditions hold on a part of the boundary $\partial\Omega_D$, and Neumann conditions hold on the remainder $\partial\Omega \setminus \partial\Omega_D$ (or indeed mixed conditions where α and β are both nonzero), see [23, 24] and the references therein.

Equation (34) can also be obtained by starting from the Lagrangian

$$L(u, u_x, u_y) = \frac{1}{2}u_x^2 + \frac{1}{2}u_y^2 - fu. \tag{36}$$

The triangle discretization of Section 4.1 in the Poisson problem defines the discrete Lagrangian

$$L_d\left(u_i^j, u_i^{j+1}, u_{i+1}^{j+1}\right) = \frac{1}{2}\Delta x \Delta y \left[\frac{1}{2}\left(\frac{u_i^{j+1} - u_i^j}{\phi(\Delta x)}\right)^2 + \frac{1}{2}\left(\frac{u_{i+1}^{j+1} - u_i^{j+1}}{\psi(\Delta y)}\right)^2\right] - \frac{f_i^j u_i^j + f_i^{j+1} u_i^{j+1} + f_{i+1}^{j+1} u_{i+1}^{j+1}}{3}. \quad (37)$$

By inserting the latter discrete Lagrangian into the discrete Euler–Lagrange field equations (22) and elaborating as done in [2], the resulting integrator from the proposed nonstandard finite difference schemes is

$$-\frac{u_i^{j+1} - 2u_i^j + u_i^{j-1}}{(\phi(\Delta x))^2} - \frac{u_{i+1}^j - 2u_i^j + u_{i-1}^j}{(\psi(\Delta y))^2} = f_i^j + \partial f_i^j / \partial u_i^j. \quad (38)$$

As a special case we chose the source term $f(x, y) \equiv 1$, so $\partial f_i^j / \partial u_i^j = 0$ in (38), and the boundary conditions $u(0, y) = u(1, y) = 0$ and $u(x, 0) = u(x, 1) = 0$. Figure 5 shows the numerical results obtained with the discretization $\Delta x = 0.02$ and $\Delta y = 0.02$.

6 Numerical Examples Using Square Discretization

To illustrate the behavior of the proposed method, we will consider the Klein–Gordon equation, which plays a significant role in many scientific applications such as solid state physics, nonlinear optics, and quantum field theory, see for example [25].

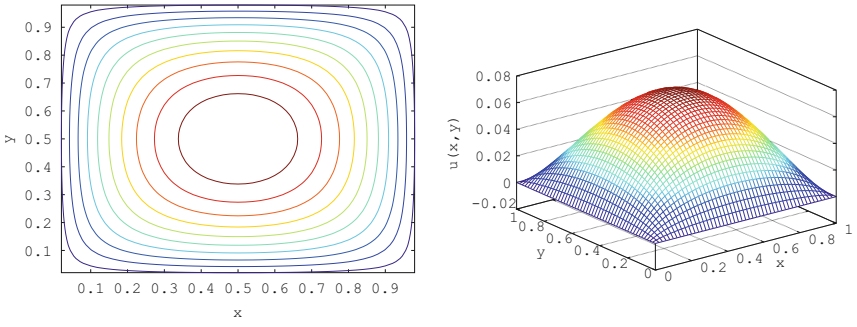

Fig. 5 Contour plot (left) and three-dimensional surface plot (right) of the solution of Poisson equation, using the variational integrator with nonstandard finite difference schemes. The source term was chosen $f(x, y) \equiv 1$, while the boundary conditions $u(0, y) = u(1, y) = 0$, $u(x, 0) = u(x, 1) = 0$ for discretization $\Delta x = 0.02$, $\Delta y = 0.02$

6.1 Klein–Gordon

For the general case, the initial-value problem of the one-dimensional nonlinear Klein–Gordon equation is given by

$$u_{tt} + \alpha u_{xx} + g(u) = f(x,t), \tag{39}$$

where $u = u(x,t)$ represents the wave displacement at position x and time t, α is a known constant and $g(u)$ is the nonlinear force which in the physical applications has also other forms [25].

Here we will consider the special case that $\alpha = -1$, $g(u) = u^3 - u$, and $f(x,t) = 0$ resulting in

$$u_{tt} = u_{xx} - u^3 + u.$$

The above equation can be described using the Lagrangian

$$L(u, u_t, u_x) = \frac{1}{2}u_t^2 - \frac{1}{2}u_x^2 - \frac{1}{4}u^4 - \frac{1}{2}u^2.$$

Following Section 4.2 we can obtain the discrete Lagrangian that now uses square discretization as

$$\begin{aligned} L_d(u_i^j, u_{i+1}^j, u_{i+1}^{j+1}, u_i^{j+1}) = {} & \frac{\Delta t \Delta x}{2}\left(\frac{u_i^{j+1} - u_i^j}{2\phi(\Delta t)} + \frac{u_{i+1}^{j+1} - u_{i+1}^j}{2\phi(\Delta t)}\right)^2 - \\ & \frac{\Delta t \Delta x}{2}\left(\frac{u_{i+1}^{j+1} - u_i^{j+1}}{2\psi(\Delta x)} + \frac{u_{i+1}^j - u_i^j}{2\psi(\Delta x)}\right)^2 - \\ & -\frac{\Delta t \Delta x}{4} u_i^j u_{i+1}^j u_{i+1}^{j+1} u_i^{j+1} + \\ & \frac{\Delta t \Delta x}{2}\left(\frac{u_i^j u_{i+1}^j + u_i^j u_{i+1}^{j+1} + u_i^j u_i^{j+1} + u_{i+1}^j u_{i+1}^{j+1} + u_{i+1}^{j+1} u_i^{j+1} + u_{i+1}^{j+1} u_i^{j+1}}{6}\right), \end{aligned}$$

which we will consider for the discrete Euler–Lagrange equations (25) in order to derive the resulting integrator from the proposed nonstandard finite difference schemes.

Figure 6 shows the numerical results obtained with the discretization $\Delta t = 0.05$ and $\Delta x = 0.05$. To that we have used initial conditions $u(x,0) = A(1 + \cos(\frac{2\pi x}{L}))$, where $A = 5$ and $u_t(x,0) = 0$, while the boundary conditions were $u(-1,t) = u(1,t)$ and $u_x(-1,t) = u_x(1,t)$.

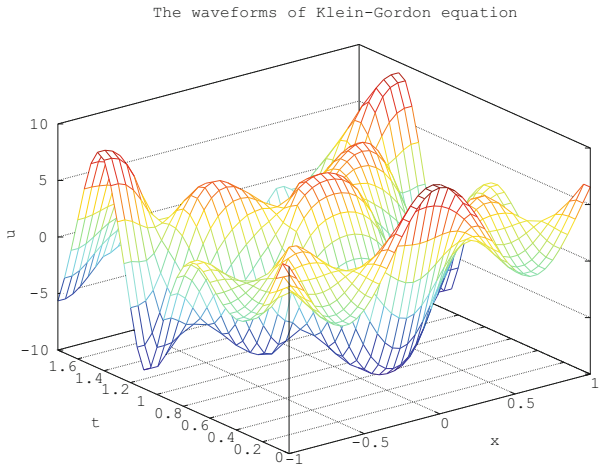

Fig. 6 Numerical solution of the Klein–Gordon equation (6.1) using square discretization of Section 4.2

7 Analysis of the Proposed Schemes

A dispersion analysis and mesh convergence experiments are performed in this section in order to show the numerical properties of the proposed method.

7.1 Dispersion Analysis

We will now turn our study to the dispersion–dissipation properties of the derived numerical schemes and compare them with the ones of [2]. To that end, similar to [26], we consider the discrete analog of the Fourier mode

$$u_i^j = \hat{u} e^{\mathbf{i}(ik\Delta x + j\omega\Delta t)}, \tag{40}$$

where $\mathbf{i}^2 = 1$. Using $\bar{k} = k\Delta x$ and $\bar{\omega} = k\Delta t$, the latter equation results in

$$u_i^j = \hat{u} e^{\mathbf{i}(i\bar{k} + j\bar{\omega})}. \tag{41}$$

Following the above, the multi-symplectic scheme of [2], also known as leapfrog algorithm, for the case of the linear wave (26) gives

$$\frac{u_i^{j+1} - 2u_i^j + u_i^{j-1}}{(\Delta t)^2} - \frac{u_{i+1}^j - 2u_i^j + u_{i-1}^j}{(\Delta x)^2} = 0. \tag{42}$$

When substituting (41) in the latter equation, we get the discrete dispersion relationship

$$\frac{e^{\mathbf{i}\bar{k}}}{(\Delta t)^2}\left[e^{2\mathbf{i}\bar{\omega}}-2e^{\mathbf{i}\bar{\omega}}+1\right]-\frac{e^{\mathbf{i}\bar{\omega}}}{(\Delta x)^2}\left[e^{2\mathbf{i}\bar{k}}-2e^{\mathbf{i}\bar{k}}+1\right]=0. \tag{43}$$

As a second example we consider the second-order implicit Runge–Kutta scheme described in [27, 28] and [29]. This scheme, also known as implicit Crank–Nicolson, is a symplectic time discretization of order two, which for the case of (26) gives

$$\begin{aligned}&4\left(u_i^{j+2}-2u_i^{j+1}+u_i^j\right)-\lambda^2\left(u_{i-1}^{j+2}-2u_i^{j+2}+u_{i+1}^{j+2}\right)\\&-2\lambda^2\left(u_{i-1}^{j+1}-2u_i^{j+1}+u_{i+1}^{j+1}\right)-\lambda^2\left(u_{i-1}^{j}-2u_i^{j}+u_{i+1}^{j}\right)=0,\end{aligned} \tag{44}$$

where

$$\lambda^2=\left(\frac{\Delta t}{\Delta x}\right)^2. \tag{45}$$

Substituting to the above integrator the form (41) we obtain the discrete dispersion relationship

$$\frac{4e^{\mathbf{i}\bar{k}}}{(\Delta t)^2}\left[e^{2\mathbf{i}\bar{\omega}}-2e^{\mathbf{i}\bar{\omega}}+1\right]-\frac{\left[e^{2\mathbf{i}\bar{k}}-2e^{\mathbf{i}\bar{k}}+1\right]}{(\Delta x)^2}\left[e^{2\mathbf{i}\bar{\omega}}-2e^{\mathbf{i}\bar{\omega}}+1\right]=0. \tag{46}$$

For the case of the linear wave equation (26) the integrator with the proposed technique, i.e., (29) for u_i^j of (41) gives

$$(\cos\bar{\omega}-1)(1-\cos\Delta x)-\left(\cos\bar{k}-1\right)(1-\cos\Delta t)=0. \tag{47}$$

For now we will restrict ourselves only to $\lambda\leq 1$, but due to symmetry, all other cases can be easily obtained. Figure 7 shows the discrete dispersion relationships for $\lambda=\{0.95, 0.9, 0.85, 0.8\}$. Specifically, to each subplot we can see the dispersion curve of the leapfrog scheme, i.e., equation (43), with blue line, the red line corresponds to the proposed method, described by (47), while the green line is the one for the implicit Runge–Kutta scheme, equation (46). For all the choices of λ tested the behavior of the method using nonstandard finite difference schemes is close to the excellent behavior of the leapfrog scheme, and much better than the implicit Runge–Kutta scheme.

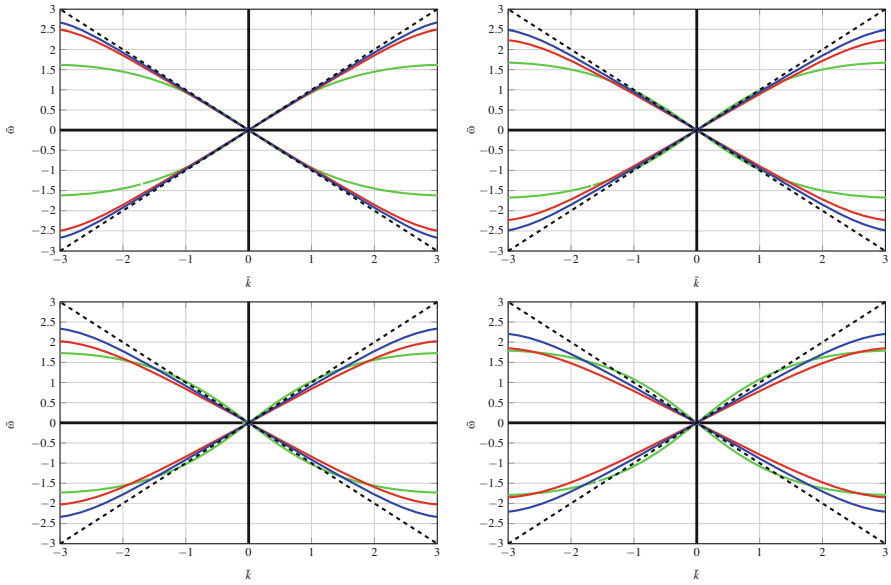

Fig. 7 Dispersion curves for the linear wave equation with the proposed method (red), the leapfrog scheme of [2] (blue), the implicit Runge–Kutta (green), and the analytic one (dashed black) for $\lambda = \{0.95, 0.9, 0.85, 0.8\}$

7.2 *Convergence Experiments*

In order to show the grid independence of the solution, following the finite element convention, the l^{∞}-norm error is calculated between the solutions on two successive grids according to

$$e_h = \max_i \{|u_i^f - u_i^c|, \ldots, |u_{n_{\text{el}}}^f - u_{n_{\text{el}}}^c|\}, \tag{48}$$

where u_i^f is the solution on the fine grid and u_i^c is the solution on a coarse grid interpolated on the fine one. Here, n_{el} are the total number of elements, where the elements of the mesh are either triangles or squares. A sample convergence of the calculations for the Klein–Gordon case is shown in Figure 8 in a logarithmic plot for triangle and square discretizations and for different time steps. It can be easily seen that by decreasing the space discretization the error is also decreased linearly in the log scale.

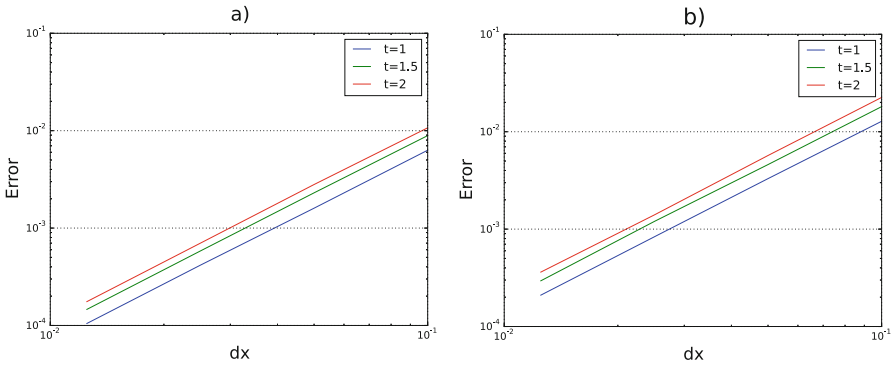

Fig. 8 Error of numerical solution as a function of grid size Δx for different time steps: (**a**) triangle discretization, (**b**) square discretization

8 Summary and Conclusions

The derivation of advantageous multi-symplectic numerical methods, relying on nonstandard finite difference schemes, is investigated. The numerical solution of the linear wave equation, the 2-D Laplace equation, and the 2-D Poisson equation, which are addressed in this study, shows a good energy behavior and the preservation of the discrete multi-symplectic structure of the proposed numerical schemes. Moreover, we showed with the help of dispersion analysis and mesh convergence experiments the numerical properties of the proposed method.

Future applications may include the field equation of incompressible fluid dynamics, like that of Cotter et al. [30] and Pavlov et al. [31], which could be of interest in investigating the properties of 3-D media. For partial differential equations arising in the field of fluid dynamics, dissipative terms should be taken into consideration. These dissipative perturbations necessitate application of techniques similar to [32, 33] but in the case of PDEs. Furthermore, a possible application in complex geometries, as they appear in real world problems, would necessitate the extension of this methodology to non-uniform grids.

The variational method presented in this work can be applied in a variety of physical problems, ranging from magnetic field simulations in NMR [34] to inverse problems that arise in geophysics [35] and others. Future work may include comparison with other numerical methods used for the solution of PDEs, such as the finite element method or the finite volume method.

Acknowledgments Dr. Odysseas Kosmas wishes to acknowledge the support of EPSRC via grand EP/N026136/1 “Geometric Mechanics of Solids.”

Appendix

By denoting $\mathrm{sinc}(\xi) = \sin(\xi)/\xi$, special cases of the exponential integrators described using (10) can be obtained, i.e.,

- Gautschi type exponential integrators [36] for

$$\psi(\Omega h) = \mathrm{sinc}^2\left(\frac{\Omega h}{2}\right), \qquad \phi(\Omega h) = 1$$

- Deuflhard type exponential integrators [37] for

$$\psi(\Omega h) = \mathrm{sinc}(\Omega h), \qquad \phi(\Omega h) = 1$$

- García-Archilla et al. type exponential integrators [38] for

$$\psi(\Omega h) = \mathrm{sinc}^2(\Omega h), \qquad \phi(\Omega h) = \mathrm{sinc}(\Omega h)$$

Finally, in [1] a way to write the Störmer–Verlet algorithm as an exponential integrators is presented.

References

1. E. Hairer, C. Lubich, G. Wanner, Geometric numerical integration illustrated by the Störmer-Verlet method. Acta Numerica **12**, 399 (2003)
2. J.E. Marsden, G.W. Patrick, S. Shkoller, Multisymplectic geometry, variational integrators, and nonlinear PDEs. Commun. Math. Phys. **199**, 351 (1998).
3. J.E. Marsden, M. West, Discrete mechanics and variational integrators. Acta Numerica **10**, 357 (2001)
4. A.P. Veselov, Integrable discrete-time systems and difference operators. Funkts. Anal. Prilozhen. **22**, 1 (1988)
5. A.P. Veselov, Integrable Lagrangian correspondences and the factorization of matrix polynomials. Funkts. Anal. Prilozhen. **25**, 38 (1991)
6. T.J. Bridges, Multi-symplectic structures and wave propagation. Math. Proc. Camb. Philos. Soc. **121**, 1 (1997)
7. T.J. Bridges, S. Reich, Multi-symplectic integrators: numerical schemes for Hamiltonian PDEs that conserve symplecticity. Phys. Lett. A **284**, 4–5 (2001)
8. T.J. Bridges, S. Reich, Numerical methods for Hamiltonian PDEs. J. Phys. **39**, 19 (2006)
9. R.E. Mickens, *Applications of Nonstandard Finite Difference Schemes* (World Scientific Publishing, Singapore, 2000)
10. R.E. Mickens, Nonstandard finite difference schemes for differential equations. J. Differ. Equ. Appl. **8**, 823 (2002)
11. R.E. Mickens, Dynamic consistency: a fundamental principle for constructing nonstandard finite difference schemes for differential equations. J. Differ. Equ. Appl. **11**, 645 (2005)
12. O.T. Kosmas, D. Papadopoulos, Multisymplectic structure of numerical methods derived using nonstandard finite difference schemes. J. Phys. Conf. Ser. **490** (2014)

13. O.T. Kosmas, Charged particle in an electromagnetic field using variational integrators. Numer. Anal. Appl. Math. **1389**, 1927 (2011)
14. O.T. Kosmas, S. Leyendecker, Analysis of higher order phase fitted variational integrators. Adv. Comput. Math. **42**, 605 (2016)
15. O.T. Kosmas, D.S. Vlachos, Local path fitting: a new approach to variational integrators. J. Comput. Appl. Math. **236**, 2632 (2012)
16. O.T. Kosmas, S. Leyendecker, Variational integrators for orbital problems using frequency estimation. Adv. Comput. Math. **45**, 1–21 (2019)
17. O.T. Kosmas, D.S. Vlachos, Phase-fitted discrete Lagrangian integrators. Comput. Phys. Commun. **181**, 562–568 (2010)
18. O.T. Kosmas, S. Leyendecker, Phase lag analysis of variational integrators using interpolation techniques. Proc. Appl. Math. Mech. **12**, 677–678 (2012)
19. O.T. Kosmas, S. Leyendecker, Stability analysis of high order phase fitted variational integrators. Proceedings of WCCM XI – ECCM V – ECFD VI, vol. 1389 (2014), pp. 865–866
20. O.T. Kosmas, S. Leyendecker, Family of high order exponential variational integrators for split potential systems. J. Phys. Conf. Ser. **574** (2015)
21. O.T. Kosmas, D.S. Vlachos, A space-time geodesic approach for phase fitted variational integrators. J. Phys. Conf. Ser. **738** (2016)
22. L. Brusca, L. Nigro, A one-step method for direct integration of structural dynamic equations. Int. J. Numer. Methods Eng. **15**, 685–699 (1980)
23. L.C. Evans, *Partial Differential Equations* (American Mathematical Society, Providence, 1998)
24. V.I. Arnold, *Lectures on Partial Differential Equations* (Springer, Berlin, 2000)
25. H. Han, Z. Zhang, Split local absorbing conditions for one-dimensional nonlinear Klein-Gordon equation on unbounded domain. J. Comput. Phys. **227**, 8992 (2008)
26. J.W. Thomas, *Numerical Partial Differential Equations*, vol. 1. Finite Difference Methods (Springer, New York, 1995)
27. J.M. Sanz-Serna, M.P. Calvo, *Numerical Hamiltonian Problems* (Chapman & Hall, London, 1994)
28. J.M. Sanz-Serna, Solving numerically Hamiltonian systems. In: *Proceedings of the International Congress of Mathematicians* (Birkhäuser, Basel, 1995)
29. S. Reich, Multi-symplectic Runge-Kutta collocation methods for Hamiltonian wave equations. J. Comput. Phys. **157**, 473 (2000)
30. C.J. Cotter, D.D. Holm, P.E. Hydon, Multisymplectic formulation of fluid dynamics using the inverse map. Proc. R. Soc. A **463**, 2671 (2007)
31. D. Pavlov, P. Mullen, Y. Tong, E. Kanso, J.E. Marsden, M. Desbrun, Structure-preserving discretization of incompressible fluids. Physica D **240**, 443 (2011)
32. E. Hairer, C. Lubich, Invariant tori of dissipatively perturbed Hamiltonian systems under symplectic discretization. Appl. Numer. Math **29**, 57–71 (1999)
33. D. Stoffer, On the qualitative behaviour of symplectic integrators. III: Perturbed integrable systems. J. Math. Anal. Appl. **217**, 521–545 (1998)
34. D. Papadopoulos, M.A. Voda, S. Stapf, F. Casanova, M. Behr, B. Blümich, Magnetic field simulations in support of interdiffusion quantification with NMR. Chem. Eng. Sci. **63**, 4694 (2008)
35. D. Papadopoulos, M. Herty, V. Rath, M. Behr, Identification of uncertainties in the shape of geophysical objects with level sets and the adjoint method. Comput. Geosci. **15**, 737 (2011)
36. W. Gautschi, Numerical integration of ordinary differential equations based on trigonometric polynomials. Numer. Math. **3**, 1 (1961)
37. P. Deuflhard, A study of extrapolation methods based on multistep schemes without parasitic solutions. Z. Angew. Math. Phys. **30**, 2 (1979)
38. B. García-Archilla, M.J. Sanz-Serna, R.D. Skeel, Long-time-step methods for oscillatory differential equations. SIAM J. Sci. Comput. **20**, 3 (1999)